Dalton Transactions **2020**, *49*, 6557-6560

https://doi.org/10.1039/D0DT01275K

COMMUNICATION

Monofunctional Platinum(II) Anticancer Complexes Based on Multidentate Phenanthridine-Containing Ligand Frameworks

Received 00th January 20xx,
Accepted 00th January 20xx

DOI: 10.1039/x0xx00000x

Issiah B. Lozada,[a] Bin Huang,[a] Morgan Stilgenbauer,[b] Travis Beach,[b] Zihan Qiu,[b] Yaorong Zheng,[b] David E. Herbert[a,†]

Phenanthriplatin is a leading preclinical anticancer Pt complex distinguished by a phenanthridine ligand that facilitates DNA-targeted covalent binding via intercalation. We report here that Pt(II) complexes incorporating phenanthridine into a chelating, multidentate ligand scaffold exhibit a superior *in vitro* therapeutic index compared with phenanthriplatin and cisplatin.

Cisplatin[1] and related platinum(II) drugs are key tools in modern cancer treatment.[2, 3] Notwithstanding its history of transformative clinical implementation, Pt chemotherapy can be limited by severe side effects caused by off-target activity and reduced efficacy due to acquired or intrinsic resistance in certain types of cancers.[4] One strategy for increasing potency and expanding the spectrum of activity of a class of compounds while mitigating side effects is to search out analogues that operate by novel mechanisms of action.[5] In this respect, monofunctional platinum anticancer complexes, a class of platin drug candidates containing only a single labile ligand first studied in earnest in the late 1980s, are attracting renewed interest.[6] Compared with bifunctional anticancer complexes such as cisplatin which deform DNA strands via formation of inter- and intrastrand crosslinks,[7] monofunctional Pt(II) complexes can only bind to DNA through a single coordination site opened up by the one vacating chloride. The antineoplastic activity of monofunctional complexes such as phenanthriplatin ([*cis*-Pt(NH_3)$_2$(phenanthridine)Cl][NO_3]; Figure 1a)[8] thus arises from different biochemical interactions compared to compounds like cisplatin (*cis*-Pt(NH_3)$_2$$Cl_2$), with a distinct spectrum of action and potential for altered resistance/side-effect profiles.

While phenanthriplatin shows heightened activity,[8] pyriplatin, in which phenanthridine is replaced with the parent *N*-heterocycle pyridine, is ten-fold *less* potent.[9] Single-molecule DNA-stretching experiments revealed a two-step binding process for phenanthriplatin, where rapid unwinding of DNA triggered by intercalation of the phenanthridine unit is followed by slower covalent modification.[10] The smaller pyridine does not associate as effectively with duplex DNA prior to covalent binding, lowering efficacy. The disposition of the *N*-heterocycle to the labile ligand is also important; DNA intercalation of the stereoisomer of phenanthriplatin with the heterocycle *trans* disposed to the chloride ([*trans*-Pt(NH_3)$_2$(phenanthridine)Cl][NO_3])[11] competes with - rather than enhancing - covalent binding, reducing the number of Pt-DNA adducts formed.[10] *Trans*-phenanthriplatin is nevertheless still an effective anticancer agent, with quite different activity compared to phenanthriplatin.[11] This is not true of *trans*platin. Covalent binding of phenanthridine to platinum to form a true monofunctional drug in phenanthriplatin also has superior activity compared with the simple combination of an intercalator such as ethidium bromide and cisplatin, which do not form a stable adduct in solution.[12]

We have recently developed synthetic mechanisms for incorporating phenanthridine into multidentate ligand architectures to explore their coordination chemistry with late

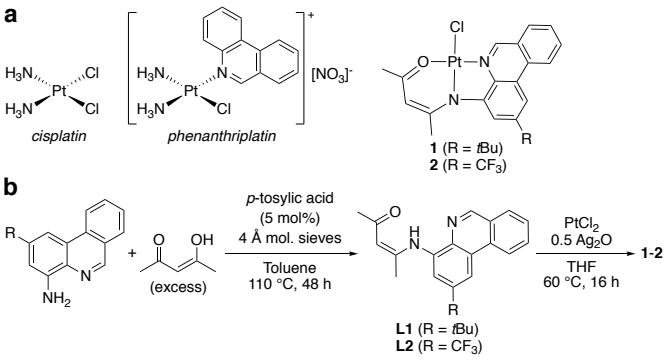

Figure 1. (a) Structures of cisplatin, phenanthriplatin[8] and the multidentate phenanthridine-ligand supported Pt complexes described herein. (b) Synthesis of chelating *N^N(H)^O* proligands **L1**-**L2** and their Pt(II) complexes **1**-**2**.

[a] *Department of Chemistry and the Manitoba Institute for Materials, University of Manitoba, 144 Dysart Road, Winnipeg, Manitoba, R3T 2N2, Canada*
[b] *Department of Chemistry, Kent State University, Kent, Ohio 44240, USA*
† david.herbert@umanitoba.ca

Electronic Supplementary Information (ESI) available: full experimental details including NMR and IR spectra, supplementary assay plots and tables, and a combined crystallographic information file. CCDC Nos. 1959703-1959704 also contain the supplementary crystallographic data for this paper, which can be obtained free of charge from The Cambridge Crystallographic Data Centre via www.ccdc.cam.ac.uk/structures. See DOI: 10.1039/x0xx00000x

transition metals.[13-15] By appending additional donors, the heterocycle can be forced *cis* to the labile chloride and exhibits a diminished tendency to dissociate irreversibly from the metal thanks to the chelate effect.[16, 17] As the attenuation of chemical reactivity and possible side effects of bifunctional platin drugs such as carboplatin and oxaliplatin are attributed in part to the stabilizing impact of chelating ligand structures,[18] we pursued the synthesis and characterization of multidentate phenanthridine-based ligands (**L1** and **L2**) and their platinum complexes (**1** and **2**, Figure 1b) to evaluate the potential of Pt(II) derivatives of chelating phenanthridine-based ligands as monofunctional chemotherapeutics. We find these chelate-supported phenanthriplatin analogs show a superior therapeutic index compared to cisplatin and phenanthriplatin *in vitro*.

Two *N^N(H)^O* proligands containing phenanthridinyl units were prepared via acid-catalyzed condensation of 4-aminophenanthridines[19] with acetylacetone (Figure 1b). The electronic influence of the substituent in the 2-position did not significantly influence the progress of the reaction. Proligands bearing electron-releasing tBu (**L1**) and electron-withdrawing CF_3 substituents (**L2**) could be isolated in similar yields (~65%). Single crystals of **L1** suitable for X-ray crystallography were grown from mixtures of diethylether and chloroform (Figure 2a). The structural metrics are consistent with a keto/enamine tautomer. In particular, the solid-state structure revealed a short C(21)-O(1) bond distance of 1.244(3) Å. This assignment was corroborated by comparing solution NMR and IR parameters with related compounds.[20] Density functional theory (DFT; RIJCOSX-PBE0/def2-TZVP) predicted IR spectra of the optimized structures of **L1** and **L2** accordingly reproduce the two notable absorptions observed experimentally between 1550-1650 cm^{-1}. The medium-strength, narrow peaks at 1617 cm^{-1} (**L1**) and 1634 cm^{-1} (**L2**) are consistent with C=O stretching modes, while the stronger absorptions at 1570 cm^{-1} (**L1**) and 1579 cm^{-1} (**L2**) are attributed to N-H bends.

Metallation of the proligands was carried out using $PtCl_2$ in the presence of 0.5 equivalents of silver oxide in THF at elevated temperatures. Again, the electronics of the phenanthridinyl unit did not impact the progress of the reaction. Platinum complexes **1** and **2** were isolated as air-stable orange solids in similar yields (~86-87%). Ligand binding was confirmed by disappearance of the downfield ^{1}H NMR signal attributed to the acidic N-*H* proton of the proligands (**L1**: 13.44 ppm; **L2**: 13.72 ppm) and a shift in the C*H* resonance in the 6-position of the phenanthridinyl ring system, which shows coupling to the ^{195}Pt nuclei in **1** and **2** (**1**: 10.03 ppm, $^3J_{PtH}$ = 39 Hz; **2**: 10.20 ppm, $^3J_{PtH}$ = 39 Hz). A similar deshielding of this particular hydrogen nucleus was observed for complexes of *bis*(phenanthridinyl)amido ligands[16] and can be interpreted as diagnostic of phenanthridinyl binding to a late transition metal. Preparations using oxygenous or nitrogenous Brönsted bases (e.g., NEt_3 or NaO*t*Bu) in place of Ag_2O were similarly successful in generating the target platinum(II) complexes. Single-crystals suitable for crystallographic analysis of **1** were also obtained. The solid-state structure (Figure 2b) reveals the co-planarity of the phenanthridinyl moiety and the coordination plane of platinum, with an angle between the two planes of 3.5°. The short C(21)-O(1) of 1.278(6) Å is consistent with retention of the keto/enamide structure upon coordination to Pt. Complexes **1** and **2** are generally soluble in organic solvents, though insoluble in aqueous media.

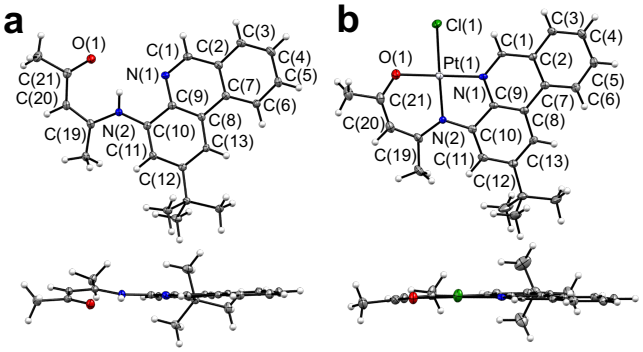

Figure 2. Two views of the solid-state structure of (a) **L1** and (b) **1** with ellipsoids shown at 30% probability. Selected bond distances (Å): **L1**: C(1)-N(1) 1.303(3), C(9)-N(1) 1.380(3), C(10)-N(2) 1.396(3), C(19)-N(2) 1.363(3), C(19)-C(20) 1.370(3), C(20)-C(21) 1.433(3), C(21)-O(1) 1.244(3). **1:** N(1)-Pt(1) 1.978(4), N(2)-Pt(1) 1.991(3), (O)-Pt(1) 1.979(3), Cl(2)-Pt(1) 2.3137(12), C(10)-N(2) 1.419(6), C(19)-N(2) 1.357(6), C(19)-C(20) 1.402(7), C(20)-C(21) 1.376(8), C(21)-O(1) 1.278(6); N(1)-Pt(1)-N(2) 82.68(14), N(1)-Pt-(1)O(1) 178.49(15), N(1)-Pt(1)Cl(2) 95.34(10), N(2)-Pt(1)-O(1) 97.61(15), N(2)-Pt(1)-Cl(1) 176.70(11), O(1)-Pt(1)-Cl(2) 84.44(11).

To assess the biological potential of chelated phenanthridine-containing monofunctional Pt(II) compounds **1** and **2**, *in vitro* cytotoxicities were evaluated using MTT assays (MTT = [3-(4,5-dimethylthiazol-2-yl)-2,5-diphenyltetrazolium bromide]; see Supporting Information). Table S1 reports IC_{50} (50% growth inhibition concentrations) for two separate ovarian cancer cell lines. The results revealed promising activity for both **1** and **2** compared with cisplatin, as well as a dependence on substituent structure. For example, **2** (R = CF_3) showed much higher *in vitro* efficacy as compared to cisplatin than **1** (R = *t*Bu), as well as less resistance than cisplatin (IC_{50} of A2780cis/IC50 of A2780) against both A2780 (cisplatin sensitive) and A2780cis (cisplatin resistant) ovarian cancer cell lines. The higher *in vitro* efficacy of **2** (R = CF_3) vs **1** (R = *t*Bu) highlights the opportunity to fine-tune biological activity via ligand backbone substitution.

In addition, neither the proligand **L2** or precursors 4-amino-(2-tert-butyl)phenanthridine or 4-amino-(2-trifluoromethyl)-phenanthridine (which may be generated upon hydrolysis of **L1** or **L2**) were found to be effective in the absence of Pt(II). The differing profile compared to cisplatin (i.e., higher *in vitro* efficacy and lower cross-resistance) implies a different mechanism of operation from cisplatin, which, considering the planar structure of **1** and **2** compared to phenanthriplatin[8] may involve a more prominent role for intercalation. As noted above, intercalation enhances covalent binding and ultimately boosts the number of complex-DNA adducts observed for phenanthriplatin, but only when these two processes are concurrent.[10] The lack of activity in the absence of Pt(II) highlights a key role for the metal centre in the cytotoxicity of **1** and **2**. Phenanthridines in general are anticipated to interact with DNA via an intercalation mechanism, similar to the

a

IC_{50} (μM)	A2780 Cisplatin-Sensitive Ovarian Cancer	A2780cis Cisplatin-Resistant Ovarian Cancer	SKOV-3 Ovarian Cancer	MDA-MB-231 Breast Cancer	A549 Lung Cancer	MET5A Mesothelial Cells	HEK-293 Human Embryonic Kidney Cells
cisplatin	1.41 ± 0.54	32.94 ± 8.82	28.60 ± 4.79	25.89 ± 20.8	34.86 ± 1.42	3.49 ± 0.86	4.99 ± 0.87
phenanthriplatin	0.17 ± 0.06	0.46 ± 0.11	1.09 ± 0.29	1.09 ± 0.22	0.137 ± 0.11	0.41 ± 0.25	4.41 ± 2.22
2	0.48 ± 0.17	0.55 ± 0.22	1.23 ± 0.06	1.11 ± 0.19	12.94 ± 3.55	1.97 ± 0.37	8.25 ± 2.18

b

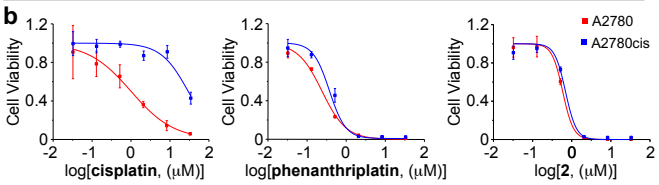

Figure 3. Cytotoxicity profiles of cisplatin, phenthriplatin, and **2** against a panel of human cancer and normal cell lines: (a) IC_{50} values, and (b) killing curves of cisplatin, phenanthriplatin, and **2** against A2780 and A2780cis ovarian cancer cells highlighting the lower resistance factor (RF) of **2**.

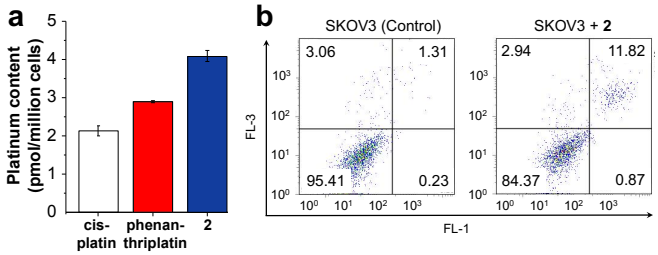

Figure 4. (a) Cellular uptake of cisplatin, phenthriplatin, and **2** in SKOV3 ovarian cancer cells ([Pt] = 2 μM, 24 h at 37 °C, 5% CO_2); (b) Annexin V/PI flow cytometric analysis of the apopotic events of SKOV3 cells with or without the treatment of **2** ([Pt] = 1 μM, 72 h at 37 °C, 5% CO_2).

mechanism of operation of the DNA stain ethidium bromide, of which phenanthridine forms the molecular core.[21] The poor activity of the aminophenanthridines excludes demetallation or hydrolysis of decoordinated proligands as the source of the observed *in vitro* anticancer activity.

With these results in hand, complex **2** was selected for further screening against additional human cancer and non-cancerous cell lines, including the non-small cell lung cancer cell line A549, ovarian cancer cell line A2780, and cisplatin-resistant ovarian cancer cell line A2780cis, ovarian cancer cell line SKOV-3, triple-negative breast cancer cell line MDA-MB-231, non-cancerous mesothelial cell line MET-5A and non-cancerous kidney cell line HEK293. Cisplatin and phenanthriplatin were used as controls. Cancerous and normal cells were treated for 72 h and cell viability was assessed. The IC_{50} values represent compound concentrations required to inhibit cell growth by 50%, and these data are tabulated in Figure 3a. Compared with cisplatin, **2** exhibits much lower IC_{50} values among all tested cell lines. For example, in A2780cis cisplatin-resistant ovarian cancer cell line, the IC_{50} (**2**) = 0.55±0.22 μM is nearly 60 times lower than that of cisplatin (IC_{50} = 32.94±8.82 μM).

Complex **2** also has comparable efficacy to phenanthriplatin across a range of cancer cell lines under the conditions tested. Importantly, however, **2** proved less toxic to normal cells (MET-5A and HEK293) compared with phenanthriplatin and displays a lower resistance factor (RF = $IC_{50(A2780cis)}/IC_{50(A2780)}$ = 1.1) in ovarian cancer cell lines than cisplatin (RF = 23) or phenanthriplatin (RF = 2.7; Figure 3b). The MTT results collectively support that the chelated monofunctional phenanthridine-based platinum compound **2** shows a superior therapeutic index compared with cisplatin and phenanthriplatin *in vitro*.

We next investigated the cellular uptake and cellular responses of **2**. First, uptake was evaluated using graphite furnace atomic absorption spectroscopy (GFAAS), with cisplatin and phenanthriplatin again employed as controls. SKOV3 cells were incubated for 24 h with 2 μM concentrations of each of the three different platinum compounds. The treated cells were then harvested and digested for GFAAS analysis. Complex **2** exhibits higher cellular uptake (4.09 ± 0.138 pmol Pt per million cells) compared with cisplatin (2.12 ± 0.129 pmol Pt per million cells) or phenthriplatin (2.88 ± 0.023 pmol Pt per million cells; Figure 4a). Similar to cisplatin,[22] phenanthriplatin uptake has been shown to be mediated by organic cation transporters (OCT); phenanthriplatin is considered a high affinity substrate for OCT2, while showing a lower apparent affinity for the multi-drug and toxin extrusion proteins (MATE) responsible for excretion of platinum into the urine.[23] Though not a cation itself, a similar affinity for transport and extrusion proteins might be plausibly expected for the chemically related **2**, as also has been observed for initially neutral platins such as cisplatin and oxaliplatin.[24] The enhanced uptake of **2** compared with phenanthriplatin does not clearly correlate with decreased cell viability for SKOV3 cells. This effect plausibly also features in the lower toxicity observed *in vitro* towards non-cancer cell lines.

With respect to cellular responses, a dual staining Annexin V/PI flow cytometry assay was used to probe the occurrence of apoptosis. In particular, SKOV3 ovarian cancer cells were treated with and without **2**. The results in Figure 4b clearly indicate that **2** induced apoptosis, stimulating SKOV3 cells to undergo early (0.87%) and late (11.82%) stage apoptosis after 72 h of incubation, the populations of which were much higher than those of control. The evidence compiled from the cell-based studies suggest that planar phenanthridine-ligated Pt(II) complexes such as **2** can readily enter cancer cells and trigger apoptosis.

Monofunctional phenanthriplatin-type complexes based on chelating tridentate *N*-heterocycle-containing ligands thus show promising *in vitro* anticancer activity, highlighting the potential of this new class of anticancer agents. The high activity towards cisplatin-resistant cancer cells is a critical finding, as tumors resistant to cisplatin often show cross-resistance to a diverse range of unrelated antitumour drugs.[25] The activation of independent pathways by the molecular structure of phenanthridine-based Pt(II) complexes similar to what is observed with phenanthriplatin[8] is likely responsible for the increased sensitivity of resistant cells to **1** and **2**.[26]

In addition, a distinguishing feature of both *cis*-phenanthriplatin and *trans*-phenanthriplatin is the orientation of the phenanthridine ligand with respect to the coordination plane of platinum. The heterocycle is nearly orthogonal in the *cis* isomer (dihedral angle ~ 89°)[8] and slightly less so in *trans*-phenanthriplatin (~ 67°).[11] Coupled with the asymmetry of phenanthridine with respect to the position of benzannulation relative to the nitrogen atom, phenanthriplatin is chiral.[27] While racemization upon rotation about the Pt-N(phenanthridine) bond is rapid enough to preclude requiring

administration of a single enantiomer, there is a preference for diastereomer formation upon binding to DNA.[27] Forcing the phenanthridinyl unit coplanar with the metal coordination plane obviates this chirality and raises the interesting question of why **1** and **2** show enhanced anticancer efficacy compared with phenanthriplatin *in vitro*. Identification of the molecular targets of **1** and **2** and investigation of potential intercalation-based mechanisms[28] therefore represent the next steps in this line of inquiry.

We are grateful for support from Research Manitoba (New Investigator Grant to DEH), the Canadian Foundation for Innovation (CFI #32146); the University of Manitoba for GETS support, the Bert & Lee Friesen Graduate Scholarship (IBML), and a Faculty of Science Undergraduate Summer Research Award (BH); and to S. McKenna and G. Tranmer for helpful discussions.

Conflicts of interest

There are no conflicts to declare.

References

1 B. Rosenberg, L. VanCamp, J. E. Trosko and V. H. Mansour, *Nature*, 1969, **222**, 385-386.
2 D. Wang and S. J. Lippard, *Nat. Rev. Drug Discov.*, 2005, **4**, 307-320.
3 B. Englinger, C. Pirker, P. Heffeter, A. Terenzi, C. R. Kowol, B. K. Keppler and W. Berger, *Chem. Rev.*, 2019, **119**, 1519-1624.
4 N. J. Wheate, S. Walker, G. E. Craig and R. Oun, *Dalton Trans.*, 2010, **39**, 8113-8127.
5 T. C. Johnstone, G. Y. Park and S. J. Lippard, *Anticancer Res.*, 2014, **34**, 471-476.
6 T. C. Johnstone, J. J. Wilson and S. J. Lippard, *Inorg. Chem.*, 2013, **52**, 12234-12249.
7 R. C. Todd and S. J. Lippard, *J. Inorg. Biochem.*, 2010, **104**, 902-908.
8 G. Y. Park, J. J. Wilson, Y. Song and S. J. Lippard, *Proc. Natl. Acad. Sci. U.S.A.*, 2012, **109**, 11987-11992, S11987/11981-S11987/11924.
9 K. S. Lovejoy, M. Serova, I. Bieche, S. Emami, M. D'Incalci, M. Broggini, E. Erba, C. Gespach, E. Cvitkovic, S. Faivre, E. Raymond and S. J. Lippard, *Mol. Cancer Ther.*, 2011, **10**, 1709-1719.
10 A. A. Almaqwashi, W. Zhou, M. N. Naufer, I. A. Riddell, Ö. H. Yilmaz, S. J. Lippard and M. C. Williams, *J. Am. Chem. Soc.*, 2019, **141**, 1537-1545.
11 W. Zhou, M. Almeqdadi, M. E. Xifaras, I. A. Riddell, Ö. H. Yilmaz and S. J. Lippard, *Chem. Commun.*, 2018, **54**, 2788-2791.
12 T. D. Tullius and S. J. Lippard, *Proc. Natl. Acad. Sci. U.S.A.*, 1982, **79**, 3489-3492.
13 R. Mondal, P. K. Giesbrecht and D. E. Herbert, *Polyhedron*, 2016, **108**, 156-162.
14 R. Mondal, I. B. Lozada, R. L. Davis, J. A. G. Williams and D. E. Herbert, *Inorg. Chem.*, 2018, **57**, 4966-4978.
15 I. B. Lozada, T. Murray and D. E. Herbert, *Polyhedron*, 2019, **161**, 261-267.
16 P. Mandapati, P. K. Giesbrecht, R. L. Davis and D. E. Herbert, *Inorg. Chem.*, 2017, **56**, 3674-3685.
17 P. Mandapati, J. D. Braun, C. Killeen, R. L. Davis, J. A. G. Williams and D. E. Herbert, *Inorganic Chemistry*, 2019, **58**, 14808-14817.
18 K. D. Mjos and C. Orvig, *Chem. Rev.*, 2014, **114**, 4540-4563.
19 J. D. Braun, I. B. Lozada, C. Kolodziej, C. Burda, K. M. E. Newman, J. van Lierop, R. L. Davis and D. E. Herbert, *Nat. Chem.*, 2019, **11**, 1144-1150.
20 R. A. M. O'Ferrall and B. A. Murray, *J. Chem. Soc., Perkin Trans. 2*, 1994, 2461-2470.
21 P. J. B. Le, *Methods Biochem Anal*, 1971, **20**, 41-86.
22 K. K. Filipski, W. J. Loos, J. Verweij and A. Sparreboom, *Clin. Cancer Res.*, 2008, **14**, 3875-3880.
23 A. Hucke, G. Y. Park, O. B. Bauer, G. Beyer, C. Koeppen, D. Zeeh, C. A. Wehe, M. Sperling, R. Schroeter, M. Kantauskaite, Y. Hagos, U. Karst, S. J. Lippard and G. Ciarimboli, *Front. Chem.*, 2018, **6**, 180/181-180/189.
24 H. Burger, W. J. Loos, K. Eechoute, J. Verweij, R. H. J. Mathijssen and E. A. C. Wiemer, *Drug Resist. Updates*, 2011, **14**, 22-34.
25 R. F. Ozols, *Hematol. Oncol. Clin. N. Am.*, **6**, 879-894.
26 Z. H. Siddik, *Oncogene*, 2003, **22**, 7265-7279.
27 T. C. Johnstone and S. J. Lippard, *J. Am. Chem. Soc.*, 2014, **136**, 2126-2134.
28 E. Y. D. Chua, G. E. Davey, C. F. Chin, P. Dröge, W. H. Ang and C. A. Davey, *Nuc. Acids Res.*, 2015, **43**, 5284-5296.

